

Mapping initial stages of localized corrosion of AA6061-T6 in diluted substitute ocean water by LEIS and SKP

Gloria Acosta, Lucien Veleva[✉]

Department of Applied Physics, Center for Research and Advanced Studies (CINVESTAV),
Unidad Mérida, km 6 Carr. Antigua a Progreso, AP 73, Cordemex, 97310 Mérida, Yucatán, México

([✉]Corresponding author: veleva@cinvestav.mx)

Submitted: 5 May 2018; Accepted: 19 July 2018; Available On-line:

ABSTRACT: Localized Electrochemical Impedance Spectroscopy (LEIS) and Scanning Kelvin Probe (SKP) maps were acquired to characterize the initial corrosion activity of 6061-T6 aluminum alloy in diluted substitute ocean water up to 24 h, simulating low polluted atmospheric environment in chlorides. Both measurements were performed *in situ* at open circuit potential. LEIS maps showed the distribution of the impedance magnitude $|Z|$ on the alloy surface, suggesting a heterogeneity in development of corrosion-active sites (first pits). SKP maps evidenced the appearance of anodic (with more negative potential) and cathodic sites on the alloy surface, which confirmed the localized character of the corrosion. SEM-EDX analysis revealed the initiation of localized aluminum dissolution in the vicinity of iron-rich intermetallic particles of Al-Fe-Si and in areas with segregated carbon, all acting as cathodes and remaining on the surface with the advance of the process.

KEYWORDS: AA6061-T6; Corrosion; LEIS; Ocean water; SKP; SEM-EDX

Citation/Citar como: Acosta, G.; Veleva, L. (2018). "Mapping initial stages of localized corrosion of AA6061-T6 in diluted substitute ocean water by LEIS and SKP". *Rev. Metal.* 54(4): e134. <https://doi.org/10.3989/revmetalm.134>

RESUMEN: *LEIS y SKP mapas de las etapas iniciales de corrosión localizada de AA6061-T6 en un sustituto de agua de mar diluido.* Mapas de Espectroscopia de Impedancia Electroquímica Localizada (LEIS) y de Sonda Kelvin de Barrido (SKP) fueron adquiridos para caracterizar las etapas iniciales de corrosión localizada de AA6061-T6 en agua de mar sustituta diluida hasta 24 h, simulando un ambiente atmosférico poco contaminado en cloruros. Ambas mediciones fueron llevadas a cabo *in situ* en potencial de circuito abierto. Los mapas de LEIS mostraron la distribución de la magnitud de la impedancia $|Z|$ en la superficie de la aleación, sugiriendo una heterogeneidad en el desarrollo de sitios activos frente a la corrosión (primeras picaduras). Los mapas de SKP evidenciaron la aparición de sitios anódicos (con potencial más negativo) y catódicos en la superficie de la aleación, lo que confirmó el carácter localizado de la corrosión. El análisis SEM-EDX reveló el inicio de la disolución de aluminio, localizado en la vecindad de partículas intermetálicas de Al-Fe-Si, ricas en hierro, y en áreas con carbono segregado, todas éstas actuando como cátodos y permaneciendo en la superficie con el avance del proceso.

PALABRAS CLAVE: AA6061-T6; Agua del océano; Corrosión; LEIS; SEM-EDX; SKP

ORCID ID: Gloria Acosta (<https://orcid.org/0000-0002-9970-7027>); Lucien Veleva (<https://orcid.org/0000-0003-1433-2885>)

Copyright: © 2018 CSIC. This is an open-access article distributed under the terms of the Creative Commons Attribution 4.0 International (CC BY 4.0) License.

1. INTRODUCTION

Aluminum alloys (AA) are applied to many fields of engineering, constructions and transportation. Typical applications of AA6061 include building materials, electrical conductor wires, packaging (foil, food and beverages), marine frames, aircraft fittings and transportations (automobiles, boats, and railroad cars) (Davis, 1999; Davis 2001). Aluminum alloys are justified by low cost, weldability, high electrical capacity and their good corrosion resistance (Staley, 1989). In the presence of oxygen in many environments having neutral pH, a thin oxide layer grows on aluminum and aluminum alloy surfaces, considered as passive film, which reduces the corrosion process. However, in the presence of reactive species, such as chlorides, localized and intergranular corrosion occur (Vera *et al.*, 1998; Szklarska-Smialowska, 1999; Braun, 2006). Corrosion initiation of AA is influenced by microstructures varied, due to the activity of intermetallic particles present in the Al-matrix, which lead to the development of local electrochemical cells (Szklarska-Smialowska, 1999; Davis, 2001; Yasakau *et al.*, 2018). Different alloying elements with limited solubility (Cu, Zn, Mg) have a considerable effect on the corrosion of the AA, which attributed to the precipitation of second-phase particles and the adjacent passive film close to them presents defects susceptible to more intensive pitting corrosion. The rate of cathodic and anodic reactions is highly dependent on the role that intermetallic particles play. Particles containing Al-Si-Mg are active sites for the nucleation of corrosion products (Guillaumin and Mankowski, 2000). The cathodic activity is associated with the Fe-containing particles, as preferential sites for oxygen reduction. And they also act as pitting initiation sites (Rynders *et al.*, 1994; Chen *et al.*, 1996). Common phases present in AA6061-T6 are: Mg₂Si, Al₂Cu, Al₃Fe, Al-Si-Mn-Fe and Al-Mg-Si (Yasakau *et al.*, 2018). Their anodic or cathodic behaviour is defined by the metallic matrix: anodic particles rich in Mg, Si and Al; and cathodic particles rich in Fe, Si and Cr (Alodan and Smyrl, 1998). Usually, the corrosion mechanism is characterized by changes in the free corrosion potential (open circuit potential) and/or the application of electrochemical techniques: electrochemical impedance spectroscopy (EIS) and polarization curves. However, they present the average of the global corrosion behaviour of the system, but cannot resolve the localized corrosion activity on the metal surface. Therefore, in recent years, localized techniques *in situ* have been developed in order to understand better the evolution of the anodic and cathodic processes at the active sites on the alloy surfaces (Annergren *et al.*, 1999).

The Scanning Kelvin Probe (SKP) technique was released in corrosion science by the Stratmann

group (Stratmann and Streckel, 1990a; Stratmann and Streckel, 1990b; Rohwerder *et al.*, 2006). SKP is a non-contact procedure, developed to evaluate the difference between conducting or semiconducting materials and a metallic probe, in terms of the surface work function (ϕ_m). The technique uses a vibrating capacitive probe and $\Delta\phi_m$ (Volta potential) is measured. In high relative humidity conditions, or in the case of a thin electrolyte layer on the metal surface, a linear dependence has been reported between the Volta potential and free corrosion potential, enabling the probe to be used for non-destructive corrosion evaluation. SKP was used to assess the localized behaviour of different aluminum alloys (Hansen *et al.*, 1999; Juzeliūnas *et al.*, 2003; Moreto *et al.*, 2014).

In order to locate precisely heterogeneities in electrodes, a novel method for generating quantitative Local Electrochemical Impedance Spectroscopy (LEIS) was developed by Isaacs's group (Lillard *et al.*, 1992). LEIS uses a similar principle of EIS: in order to calculate the impedance, a small sinusoidal voltage perturbation is applied to a specimen surface and the resulting current in the immediate vicinity of working the electrode surface is measured. This technique has been carried out to research, for example, the degradation of organic coatings and coating defects (Zou and Thierry, 1997), the kinetics of initiation and propagation of pit (Annergren *et al.*, 1999). Some recent developments of LEIS have been reported (Huang *et al.*, 2011; Orazem and Tribollet, 2017).

The distribution of the intermetallic particles in the alloy matrix is the principal aspect when the localized corrosion process is studied. The corrosion process of AA6061-T6, considered in this work, was characterized in the presence of thin aqueous layers on the surface, containing low chloride ion concentration within a millimolar range of NaCl, as atmospheric marine environment in which might alloy be exposed. For this reason, LEIS and SKP *in situ* experiments were performed in diluted substitute ocean water (0.035% salinity, 4.2 mM NaCl). The present work focuses on the characterization of the initial stages of the electrochemical activity on an aluminum alloy 6061-T6 surface, in this model electrolyte up to 24 h. The resulting maps provided useful information *in situ* for the localized corrosion process at AA6061-T6 surface. The results have been supported by SEM-EDX analysis of the alloy surface.

2. MATERIALS AND METHODS

For the present research, aluminum alloy 6061-T6 was used and its nominal composition (wt. %), according to Metal Plastic Mexicali is: 1.10% Mg, 0.5% Fe, 0.31% Cu, 0.19% Cr, 0.07% Zn, 0.07% Si, 0.03% Ti and the remainder Al. Specimens of 1 cm² size have been prepared as working electrodes.

Before experiments, the alloy surface was degreased with ethanol.

Substitute ocean water was prepared with deionized water and analytical grade reagents in accordance with the norm ASTM D1141-98 (2008). This water was diluted in the ratio 1:100 (conductivity = $736 \mu\text{S}\cdot\text{cm}^{-1}$, pH = 6.2, T = 20 °C) and denominated “diluted substitute ocean water” (4.2 mM NaCl). Both techniques, LEIS and SKP, enabled greater resolution to be achieved in diluted solutions with low ionic concentration; they also match well with the very small current densities expected at the beginning of the alloy surface corrosion activity. The working electrodes of AA6061-T6 were immersed in 10 mL of model electrolyte. LEIS and SKP experiments have been performed after 1, 3, 6, 9, 12 and 24 h of exposure of the alloy in the electrolyte.

2.1. SEM-EDX

The AA6061-T6 specimens were withdrawn after LEIS and SKP measurements and their surfaces were analyzed. Images of the alloy surface morphology and its elemental composition were provided by scanning electron microscopes (SEM-EDX, Phillips XL-30 and ESEM JEOL JSM-7600 F). Subsequently, the corrosion products were chemically removed from the surface in HNO_3 (1.42 g mL^{-1}) during 5 min at 25 °C, according to ISO 8407 (1991) and their surfaces were again observed with SEM and EDX techniques.

2.2. Corrosion test

The LEIS tests were performed with the scanning electrochemical workstation (Model 370), including a Potentiostat/Galvanostat/FRA (Model 3300) and a video camera system to guarantee that the micro probe was very close to the specimen surface with a five-electrode configuration. The working electrode was an AA6061-T6 specimen, while Ag/AgCl electrode acted as reference electrode and platinum wire as the counter electrode. LEIS micro-probe was a Pt bi-electrode, moved in three axes to adjust over the surface of the WE at 50 μm , to quantify the local potential gradient in the solution between the alloy surface and the probe, which then was linked with the local AC-current density $i_{loc}(\omega)$ flowing in the system, obtained through the Ohm’s law (Huang *et al.*, 2007) Eq. (1):

$$i_{loc}(\omega) = \frac{\Delta V_{probe}(\omega)}{d} \times k \quad (1)$$

where k is the electrolyte conductivity, $\Delta V_{probe}(\omega)$ - the AC-potential gradient between the two probes and d - the distance between the two probes. The value of z_{local} implies that the electrode potential is

quantified as a function of the reference electrode, situated well inside the bulk of the solution, Eq. (2):

$$z_{local}(\omega) = \frac{\tilde{V}(\omega) - \phi_{ref}}{i_{loc}(\omega)} = \frac{\Delta \tilde{V}(\omega)}{\Delta V_{probe}(\omega)k} \quad (2)$$

Here $\tilde{V}(\omega) - \phi_{ref}$ represents the variation of the AC-potential, along the distance that separates the electrode surface and the reference electrode in the bulk solution.

An AC disturbance amplitude of 10 mV was applied to the WE at open circuit. LEIS maps were obtained by scanning an area of $500 \times 400 \mu\text{m}$ in the x-y direction, with a step size of $20 \mu\text{m}\cdot\text{s}^{-1}$. The data were plotted using 3DIsoplot software which allows the acquisition of 3D and 2D plots. The local AC-current density i_{loc} was acquired according to Ohm’s law (Huang *et al.*, 2007). The excitation frequency chosen was 700 Hz, after previous access to EIS diagrams data, considered as the initiation of the corrosion process.

Home-made SKP equipment was used in this research. The reference electrode composed a 80Ni-20Cr alloy needle with a tip diameter of 50 μm , which was moved in x, y and z direction. All scans were fully automated. The probe potential was calibrated with respect to a copper/copper sulfate (Cu/CuSO₄) electrode. The free corrosion potential values are given *versus* the standard hydrogen electrode (SHE). The distance between the tip and the alloy surface was 150 μm during all experiments, with height control. After the exposure of the working electrodes in the model electrolyte for different periods of time, they were removed and placed into a SKP experimental camera, with the relative humidity kept at 95% and temperature of 20 °C. The scanned surface was $2000 \times 1000 \mu\text{m}$ with a step of 20 μm , in the x-y direction.

3. RESULTS AND DISCUSSION

3.1. SEM-EDX analysis

SEM image of the microstructure of the 6061-T6 aluminum alloy is shown in Fig. 1a. In agreement with the literature (Yasakau *et al.*, 2018) EDX analysis (Table 1) revealed the composition of several intermetallics: iron-rich (Al-Fe-Si, particle A), magnesium-rich (Mg-Si, particle B), and Al-Cu (particles C), forming second-phases, which make AA6061-T6 susceptible to localized corrosion.

After 24 h of immersion of AA6061-T6 in diluted substitute ocean water the surface was covered partially by a corrosion layer, observable as “black” spots (Fig. 1b) and according to EDX analysis (Table 1, Fig. 1b) the composition thereof might correspond to aluminum oxide or hydroxide. It may be noted that in these spotted areas EDX

TABLE 1. SEM-EDX analysis of AA6061-T6 surface (Fig. 1)

Element (wt.%)	(a) A	(a) B	(a) C	(b) 1	(b) A	(c) A	(c) B
C	–	2.93	–	19.01	10.02	4.41	5.43
O	2.70	3.64	2.26	24.57	10.15	2.68	4.12
Mg	0.61	2.86	0.36	0.77	0.72	0.30	1.56
Al	76.27	88.92	26.43	55.38	62.13	68.45	87.59
Si	3.92	1.18	–	0.28	3.54	5.09	0.91
Cr	0.50	–	–	–	–	0.75	–
Mn	0.92	–	–	–	0.69	1.12	–
Fe	14.39	0.47	–	–	12.11	16.21	0.39
Cu	0.69	–	61.95	–	0.64	1.00	–

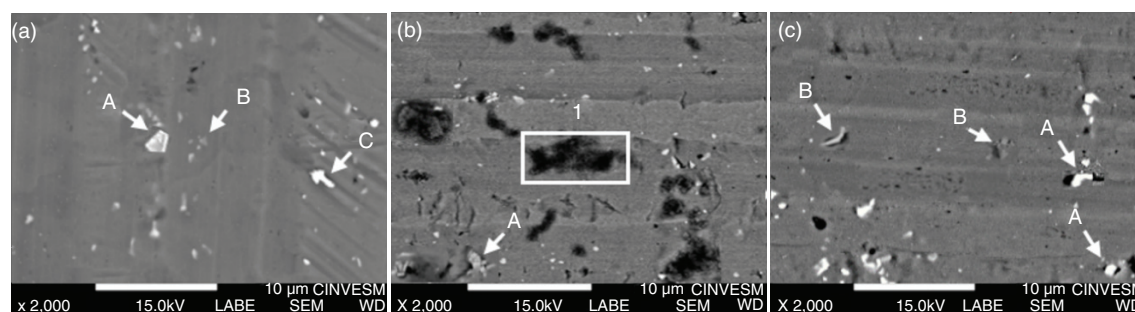


FIGURE 1. SEM-EDX images of AA6061-T6: (a) reference sample; (b) after 24 h of exposure in diluted substitute ocean water, and (c) after removal of corrosion products.

reveals the presence of segregated carbon, which has served as a cathode in the vicinity of anodic active Al-matrix (Table 1, Fig. 1b). It was also observed that the intermetallic iron-rich particles (Table 1, Fig. 1a - particle A), serving as cathodes, remain on the surface. It is reported that around them a preferential dissolution of the aluminum matrix was initiated (Rynders *et al.*, 1994; Chen *et al.*, 1996). After removal of the corrosion layer, the micrograph in Fig. 1c shows the localized pitting attacks on the alloy surface after 24 h of exposure in diluted ocean water and the presence of the intermetallics “A” (iron-rich) and “B” (Al-Mg-Si), cathodic and anodic particles, respectively. It is considered that the first pitting starts within seconds of exposure in Cl-containing solutions, probably due to the dissolution of Mg, as a part of the Mg-Si phase (Eckermann *et al.*, 2008).

3.2. LEIS measurements

Figure 2 illustrates the LEIS maps 3D and 2D, obtained for the 6061-T6 aluminum alloy at the initial time of up to 24 h of exposure in diluted substitute ocean water. In accordance with $|Z|$ magnitude, the gradient of colours goes from blue

to red. With the advance of the corrosion process, i.e. time of exposure of AA6061-T6 in diluted substitute ocean water, the colour intensity characterizes the distribution of impedance on the sample surface, therefore, the heterogeneity, due to the development of corrosion-active sites (first pits) in the presence of chloride ions, which break down the passive layer formed in air on aluminum alloy. The $|Z|$ magnitude decreases in the first six hours (Fig. 2 a-c) from $6.48 \text{ M}\Omega\cdot\text{cm}^2$ to $3.01 \text{ M}\Omega\cdot\text{cm}^2$, as a consequence of the intensive development of localized pitting events and the passive layer rupture. However, in the second period of time (Fig. 2 d-e) the magnitude of $|Z|$ maintains almost a similar value ($2.32 - 2.11 \text{ M}\Omega\cdot\text{cm}^2$, at 9 and 12 h of exposure, respectively). This fact suggests a quasi-stationary corrosion process, when the ion migration through the corrosion layer delays the advance of pit formation (Burstein *et al.*, 2004). The shift of the magnitude of $|Z|$ to $3.24 \text{ M}\Omega\cdot\text{cm}^2$ at 24 h (the end of this experiment) was attributed to surface sites covered partially by a corrosion layer, observable as “black” spots (Fig. 1b); the EDX was presented in Table 1 (Fig. 1b). However, the localized corrosion process continues (lower values of magnitude of $|Z|$), owing to cracking

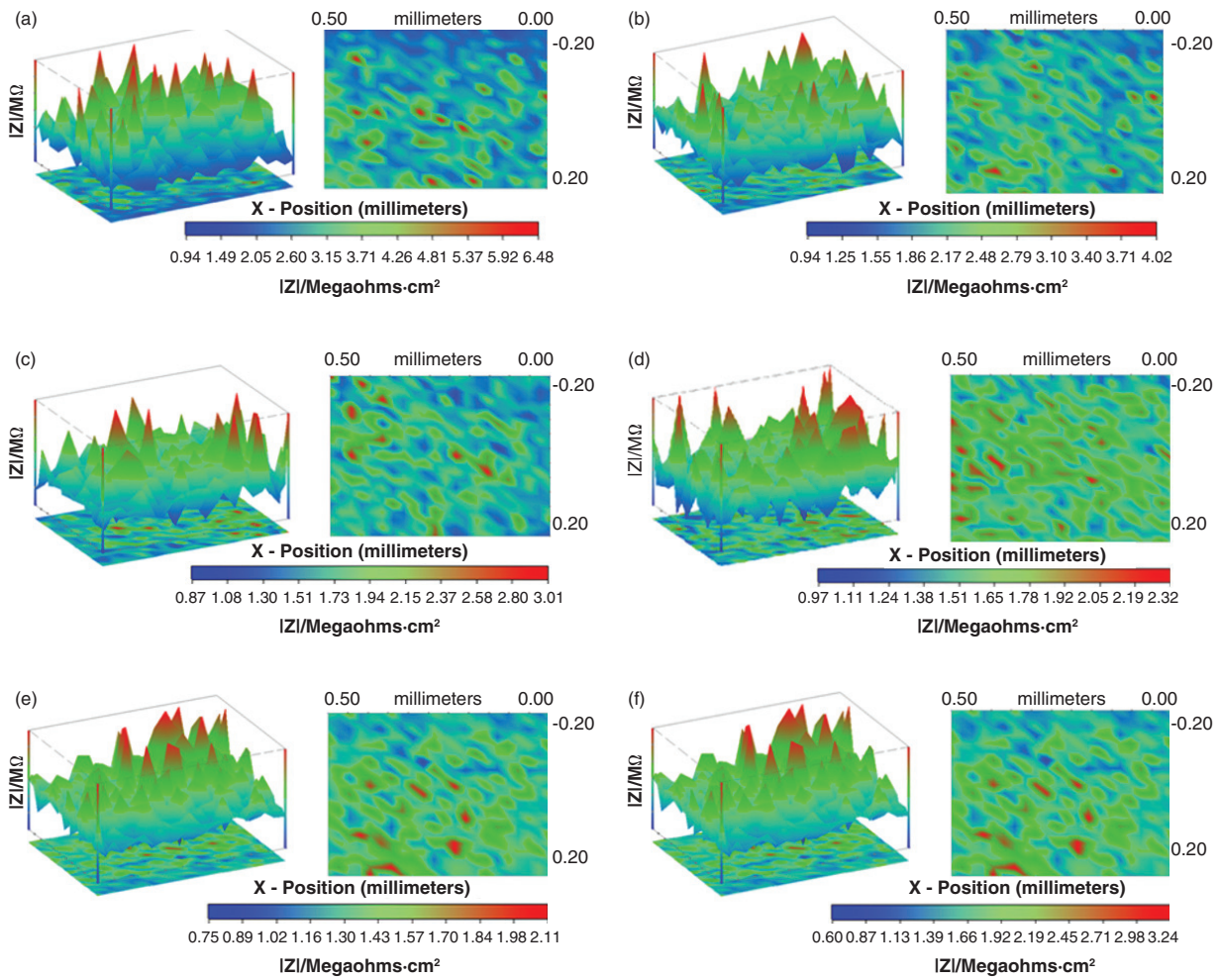


FIGURE 2. The 3D and 2D maps of LEIS measurements on AA6061-T6 surface: a) 1 h, b) 3 h, c) 6 h, d) 9 h, e) 12 h and f) 24 h of exposure in diluted substitute ocean water.

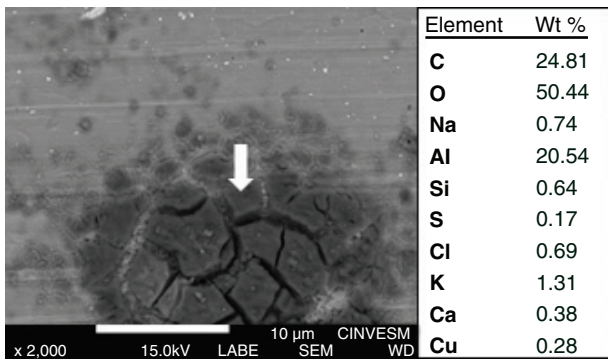


FIGURE 3. SEM-EDX of AA6061-T6 after 24 h of LEIS measurements in diluted ocean water.

of the corrosion layer and formation of new pits (Fig. 3).

EDX analysis (Fig. 3) suggested that the composition of the cracked corrosion layer corresponds to aluminum oxide or hydroxide, formed on the area of

segregated carbon, which served as cathode in the vicinity of the active Al-matrix.

3.3. SKP maps

The potential maps, acquired by SKP for the AA6061-T6 in diluted substitute ocean water, performed at different times (1 h up 24 h), are shown in Fig. 4. These maps evidence the heterogeneous appearance of localized anodic (increased negative potential) and cathodic sites on the alloy surface. In the first six hours (Fig. 4 a-c), the more active anodic sites revealed potential values up to -0.669 V. This fact confirms the formation of the first pits in the alloy surface, as LEIS maps suggested (Fig. 2), due to the breakdown of the natural passive layer with the attack of the chloride ions. After this period of time, the potential value tends to be less negative, when the corrosion layer starts to cover the surface, reaching a positive value of around 0.354 V (Fig. 4f) at 24 h of exposure, and the electrochemical activity declines.

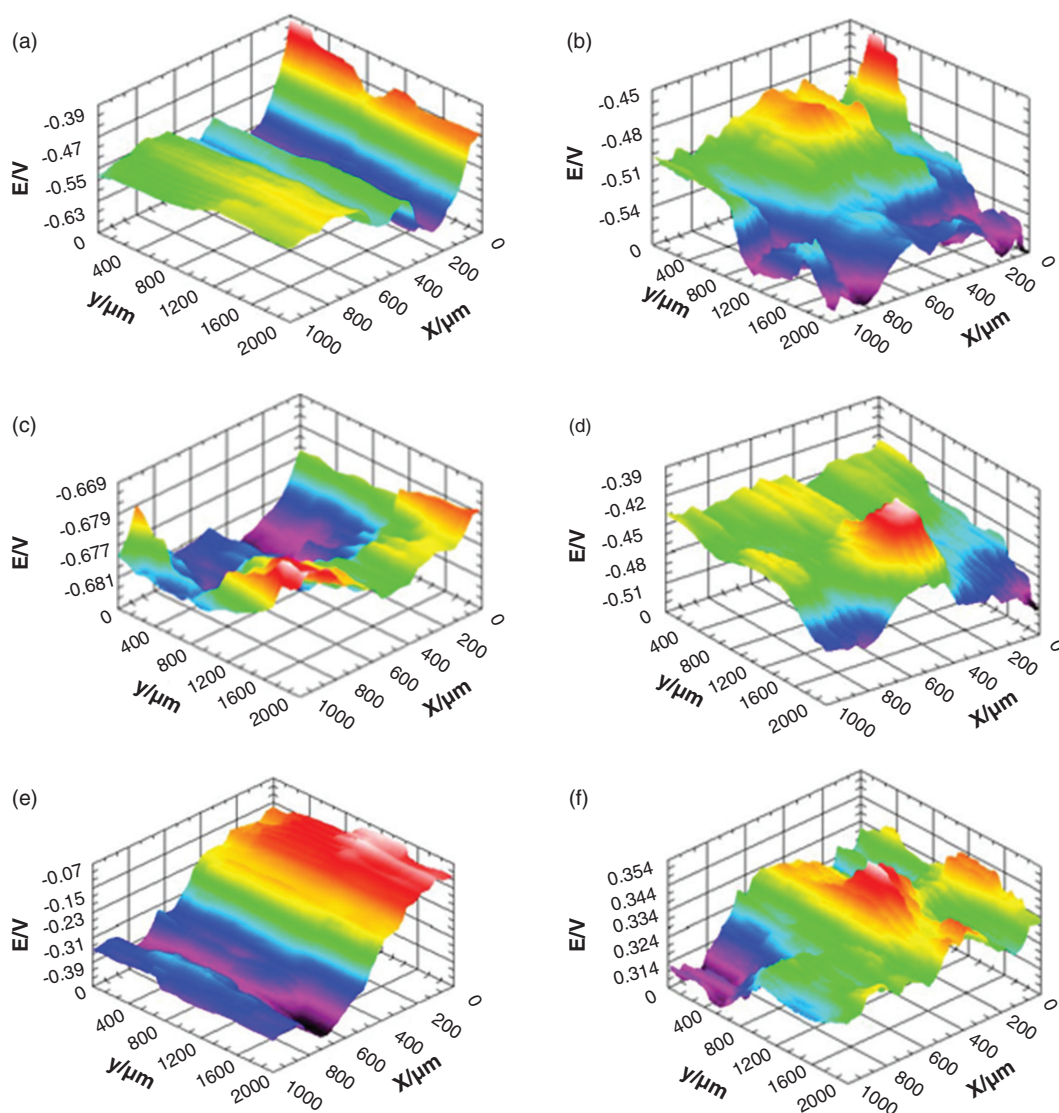


FIGURE 4. SKP maps representing free corrosion potential distribution (E vs SHE) on AA6061-T6 surface: a) 1 h, b) 3 h, c) 6 h, d) 9 h, e) 12 h and f) 24 h of exposure in diluted substitute ocean water.

4. CONCLUSIONS

- In order to probe the local activity of AA6061-T6 surface and the initiation of corrosion, local electrochemical impedance spectroscopy (LEIS) and scanning Kelvin probe microscopy (SKP) maps were employed. As a model solution diluted substitute ocean water was used, simulating a low polluted atmospheric environment in chlorides.
- In accordance with the impedance $|Z|$ magnitude distribution on the alloy surface, with the advance of the time of exposure of AA6061-T6 a heterogeneous activity was observed, due to the development of corrosion-active sites (first pits) in the presence of chloride ions, which break down the passive layer formed in air on aluminum alloy.
- From the potential maps acquired by SKP, it was evident that more active sites have more negative potential, considered as local anodes.
- The additional SEM-EDX information suggested that the preferential dissolution of Al occurs in the vicinity of iron-rich intermetallic particles of Al-Fe-Si and in areas with segregated carbon, all acting as cathodes and remaining on the surface with the advance of the process.

ACKNOWLEDGMENTS

Gloria Acosta wishes to thank CONACYT for the scholarship granted for her Ph. D. study and for the research stay at the National Centre for Metallurgical Research (CENIM, CSIC), Madrid, Spain. This research was funded by CONACYT grant project No. 179110. The authors are grateful to M. Sci. Dora Huerta for her assistance in SEM-EDX acquisition images.

REFERENCES

- Alodan, M., Smyrl, W. (1998). Detection of localized corrosion of aluminum alloys using fluorescence microscopy. *J. Electrochem. Soc.* 145 (5), 1571–1577. <https://doi.org/10.1149/1.1838520>.
- Annergren, I., Zou, F., Thierry, D. (1999). Application of localized electrochemical techniques to study kinetics of initiation and propagation during pit growth. *Electrochim. Acta* 44 (24), 4383–4393. [https://doi.org/10.1016/S0013-4686\(99\)00154-1](https://doi.org/10.1016/S0013-4686(99)00154-1).
- ASTM D1141-98 (2008). Standard practice for the preparation of substitute ocean water. ASTM, West Conshohocken.
- Braun, R. (2006). Investigation on microstructure and corrosion behaviour of 6XXX series aluminium alloys. *Mater. Sci. Forum* 519–521, 735–740. <https://doi.org/10.4028/www.scientific.net/MSF.519-521.735>.
- Burstein, G.T., Liu, C., Souto, R.M., Vines, S.P. (2004). Origins of pitting corrosion. *Corros. Eng. Sci. Techn.* 39 (1), 25–30. <https://doi.org/10.1179/147842204225016859>.
- Chen, G.S., Gao, M., Wei, R.P. (1996). Microconstituent-induced pitting corrosion in aluminum alloy 2024-T3. *Corrosion* 52 (1), 8–15. <https://doi.org/10.5006/1.3292099>.
- Davis, J.R. (1999). *Corrosion of aluminum and aluminum alloys*. ASM International, Materials Park, Ohio, USA.
- Davis, J.R. (2001). *Aluminum and aluminum alloys*. In *Alloying: Understanding the basics*. ASM International, Materials Park, Ohio, USA.
- Eckermann, F., Suter, T., Uggowitz, P.J., Afseth, A., Schmutz, P. (2008). The influence of MgSi particle reactivity and dissolution processes on corrosion in Al–Mg–Si alloys. *Electrochim. Acta* 54 (2), 844–855. <https://doi.org/10.1016/j.electacta.2008.05.078>.
- Guillaumin, V., Mankowski, G. (2000). Localized corrosion of 6056 T6 aluminium alloy in chloride media. *Corros. Sci.* 42 (1), 105–125. [https://doi.org/10.1016/S0010-938X\(99\)00053-0](https://doi.org/10.1016/S0010-938X(99)00053-0).
- Hansen, D.C., Grecsek, G.E., Roberts, R.O. (1999). *A scanning kelvin probe analysis of aluminum and aluminum alloys*. Corrosion '99, NACE International, San Antonio, Texas.
- Huang, V.M.W., Vivier, V., Orazem, M.E., Pebere, N., Tribollet, B. (2007). The apparent constant-phase-element behavior of an ideally polarized blocking electrode. *J. Electrochem. Soc.* 154 (2), C81–C88. <https://doi.org/10.1149/1.2398882>.
- Huang, V.M.W., Wu, S-L., Orazem, M.E., Pèbère, N., Tribollet, B., Vivier, V. (2011). Local electrochemical impedance spectroscopy: A review and some recent developments. *Electrochim. Acta* 56 (23), 8048–8057. <https://doi.org/10.1016/j.electacta.2011.03.018>.
- ISO 8407 (1991). Corrosion of metals and alloys - Removal of corrosion products from corrosion test specimens, International Organization for Standardization, Genève.
- Juzeliūnas, E., Leinartas, K., Fürbeth, W., Jüttner, K. (2003). Study of initial stages of Al–Mg alloy corrosion in water, chloride and Cu(II) environment by a scanning Kelvin probe. *Corros. Sci.* 45 (9), 1939–1950. [https://doi.org/10.1016/S0010-938X\(03\)00026-x](https://doi.org/10.1016/S0010-938X(03)00026-x).
- Lillard, R.S., Moran, P.J., Isaacs, H.S. (1992). A novel method for generating quantitative local electrochemical impedance spectroscopy. *J. Electrochem. Soc.* 139 (4), 1007–1012. <https://doi.org/10.1149/1.2069332>.
- Moreto, J.A., Marino, C.E.B., Bose Filho, W.W., Rocha, L.A., Fernandes, J.C.S. (2014). SVET, SKP and EIS study of the corrosion behaviour of high strength Al and Al-Li alloys used in aircraft fabrication. *Corros. Sci.* 84, 30–41. <https://doi.org/10.1016/j.corsci.2014.03.001>.
- Orazem, M.E., Tribollet, B. (2017). *Local electrochemical impedance spectroscopy*. In: *Electrochemical Impedance Spectroscopy*. J. Wiley & Sons, Inc., New Jersey, USA.
- Rohwerder, M., Stratmann, M., Leblanc, P., Frankel, G.S. (2006). *Application of scanning Kelvin probe in corrosion science*. In: *Analytical methods in corrosion science and engineering*. Chapter 16, Edited by P. Marcus, F. Mansfeld, Taylor & Francis Group, USA, pp. 606–648.
- Rynders, R.M., Paik, C.H., Ke, R., Alkire, R.C. (1994). Use of in situ atomic force microscopy to image corrosion at inclusions. *J. Electrochem. Soc.* 141 (6), 1439–1445. <https://doi.org/10.1149/1.2054943>.
- Staley, J.T. (1989). *Treatise on Materials Science and Technology. Aluminium alloys-contemporary research and applications*. Vol. 31, Edited by Vasudevan, A.K., Doherty, R.D., Academic Press, Boston.
- Stratmann, M., Streckel, H. (1990a). On the atmospheric corrosion of metals which are covered with thin electrolyte layers-I Verification of the experimental technique. *Corros. Sci.* 30 (6–7), 681–696. [https://doi.org/10.1016/0010-938X\(90\)90032-Z](https://doi.org/10.1016/0010-938X(90)90032-Z).
- Stratmann, M., Streckel, H. (1990b). On the atmospheric corrosion of metals which are covered with thin electrolyte layers-II Experimental results. *Corros. Sci.* 30 (6–7), 697–714. [https://doi.org/10.1016/0010-938X\(90\)90033-2](https://doi.org/10.1016/0010-938X(90)90033-2).
- Szklarska-Smialowska, Z. (1999). Pitting Corrosion of Aluminum. *Corros. Sci.* 41 (9), 1743–1767. [https://doi.org/10.1016/S0010-938X\(99\)00012-8](https://doi.org/10.1016/S0010-938X(99)00012-8).
- Vera, R., Schrebler, R., Layana, G., Orellana, F., Olguín, A. (1998). Corrosión por picaduras del aluminio y de la aleación Al-6201 en soluciones de NaCl. *Rev. Metal.* 34 (3), 268–273. <https://doi.org/10.3989/revmetalm.1998.v34.i3.793>.
- Yasakau, K.A., Zheludkevich, M.L., Ferreira, M.G.S. (2018). *Role of intermetallics in corrosion of aluminum alloys*. *Smart corrosion protection*. In: *Intermetallic Matrix Composites, Properties and Applications*. Woodhead Publishing, Aveiro, Portugal, pp. 425–462.
- Zou, F., Thierry, D. (1997). Localized electrochemical impedance spectroscopy for studying the degradation of organic coatings. *Electrochim. Acta* 42 (20–22), 3293–3301. [https://doi.org/10.1016/S0013-4686\(97\)00180-1](https://doi.org/10.1016/S0013-4686(97)00180-1).